

Supporting information

Key Role of Metal-to-Metal Charge Transfer Transition between Mo^{6+} and Bi^{3+} for Enhancement in NIR Luminescence of $\text{Gd}_2\text{MoO}_6\text{:Bi,Yb}$ Nanophosphor

Taisei Hangai,¹ Takuya Hasegawa,^{*,1} Jian Xu,² Takayuki Nakanishi,³ Takashi Takeda,³ Kosuke Nakano,⁴ Kenta Hongo,⁴ Ryo Maezono,⁴ Tomoyo Goto,^{5,6} Yasushi Sato,⁷ Ayahisa Okawa,¹ and Shu Yin^{1,8}

¹ Institute of Multidisciplinary Research for Advanced Material (IMRAM), Tohoku University, 2-1-1 Katahira, Aoba-ku, Sendai, 980-8577, Japan

² International Center for Young Scientists (ICYS), National Institute for Materials Science (NIMS), Tsukuba, Ibaraki 305-0044, Japan

³ Advanced Phosphor Group, National Institute for Materials Science (NIMS), Tsukuba, Ibaraki, 305-0044, Japan

⁴ School of Information Science, Japan Advanced Institute of Science and Technology (JAIST), Asahidai 1-1, Nomi, Ishikawa 923-1292, Japan

⁵ SANKEN (The Institute of Scientific and Industrial Research), Osaka University, 8-1 Mihogaoka, Ibaraki, Osaka 567-0047, Japan

⁶ Institute for Advanced Co-Creation Studies, Osaka University, 1-1 Yamadaoka, Suita, Osaka, 565-0871, Japan

⁷ Department of Chemistry, Faculty of Science, Okayama University of Science, 1-1 Ridai-cho, Kita-ku, Okayama 700-0005, Japan

⁸ Advanced Institute for Materials Research (WPI-AIMR), Tohoku University, Sendai 980-8577, Japan

*Corresponding author:

Takuya Hasegawa: hase@tohoku.ac.jp

Figure and Table content

Figure S1. Narrow scan analysis of XPS for (a) Gd 4d, and (b) Mo 3d for all GMO nanophosphors

Figure S2. XANES spectra for all GMO nanophosphors of (a) Gd L_{3-} , (b) Mo $K-$, (c) Bi L_{3-} , and (d) Yb L_{3-} edge with the reference samples (Gd_2O_3 , MoO_3 , Bi_2O_3 , and Yb_2O_3).

Figure S3. TG-DTA curve for GMO:Bi,Yb, and from 330 K to 1000 K under ambient air.

Figure S4. ΔE values calculated by the total energy obtained after structural relaxation.

Figure S5. Fourier transformed EXAFS radial distribution function spectra of Mo K -edge in all GMO nanophosphors.

Figure S6. (a)DOS/pDOS of GMO:Bi substituted in Gd3 site, and (b) enlarged one.

Figure S7. Kubelka-Munk spectra of all GMO nanophosphors around 500 nm.

Figure S8. Decay curve of GMO:Yb and GMO:Bi,Yb at 300 K ($\lambda_{ex}= 360$ nm and $\lambda_{em}= 975$ nm).

Figure S9. (a) PL spectra ($\lambda_{ex}= 363$ nm) and (b) decay curve ($\lambda_{ex}= 360$ nm and $\lambda_{em}= 975$ nm) of GMO:Bi, $_y$ Yb ($y = 5, 7, 8, 9,$ and 10 mol%) nanophosphors at 300 K.

Figure S10. Gaussian fit of the PLE spectra ($\lambda_{em}= 670$ nm) for GMO and GMO:Bi at 77 K.

Figure S11. (a) PL spectra ($\lambda_{ex}= 360$ nm) and (b) integrated intensity of GMO: $_x$ Bi, ($x = 0, 0.5, 1, 2,$ and 3 mol%) nanophosphors at 77 K.

Figure S12. Enlarged DOS/pDOS of GMO:Bi substituted in Gd1 around conduction band minimum.

Table S1. Molar ratios of Gd/Bi/Yb for all GMO nanophosphors calculated from XPS.

Table S2. Lattice parameters for each GMO nanophosphor refined by Rietveld analysis.

Table S3. Lattice parameters and bond length between cation (Gd, Mo) and oxygen obtained from optimized by DFT, Rietveld refined, and CIF.

Table S4. Calculated total energy after structural relaxation and ΔE values.

Table S5. Fitting parameters of decay curves for GMO:Yb and GMO:Bi,Yb measured at 300 K.

Table S6. Fitting parameters of decay curves for GMO:Bi, $_y$ Yb ($y = 5, 7, 8, 9,$ and 10 mol%) nanophosphors measured at 300 K ($\lambda_{ex}= 360$ nm and $\lambda_{em}= 975$ nm).

Table S7. Fitting parameters of decay curves for GMO:Bi, y Yb ($y = 0, 0.5,$ and 1 mol%) nanophosphors measured at 77 K ($\lambda_{\text{ex}} = 360$ nm and $\lambda_{\text{em}} = 670$ nm).

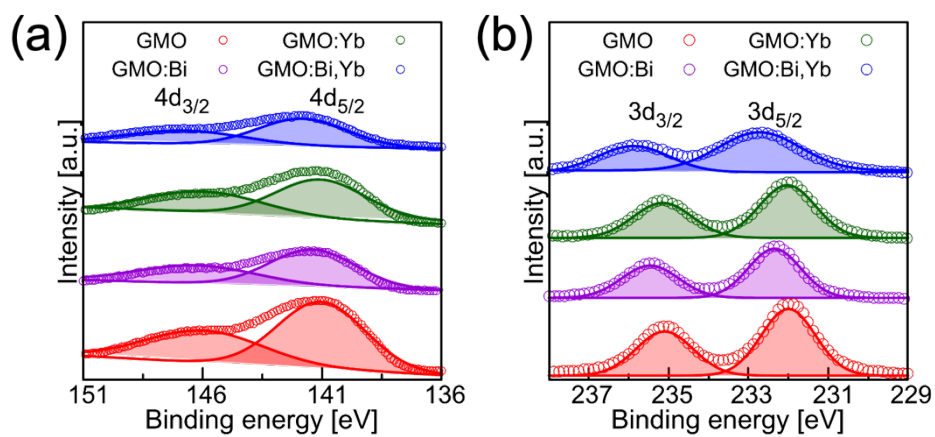


Figure S1. Narrow scan analysis of XPS for (a) Gd 4d and (b) Mo 3d.

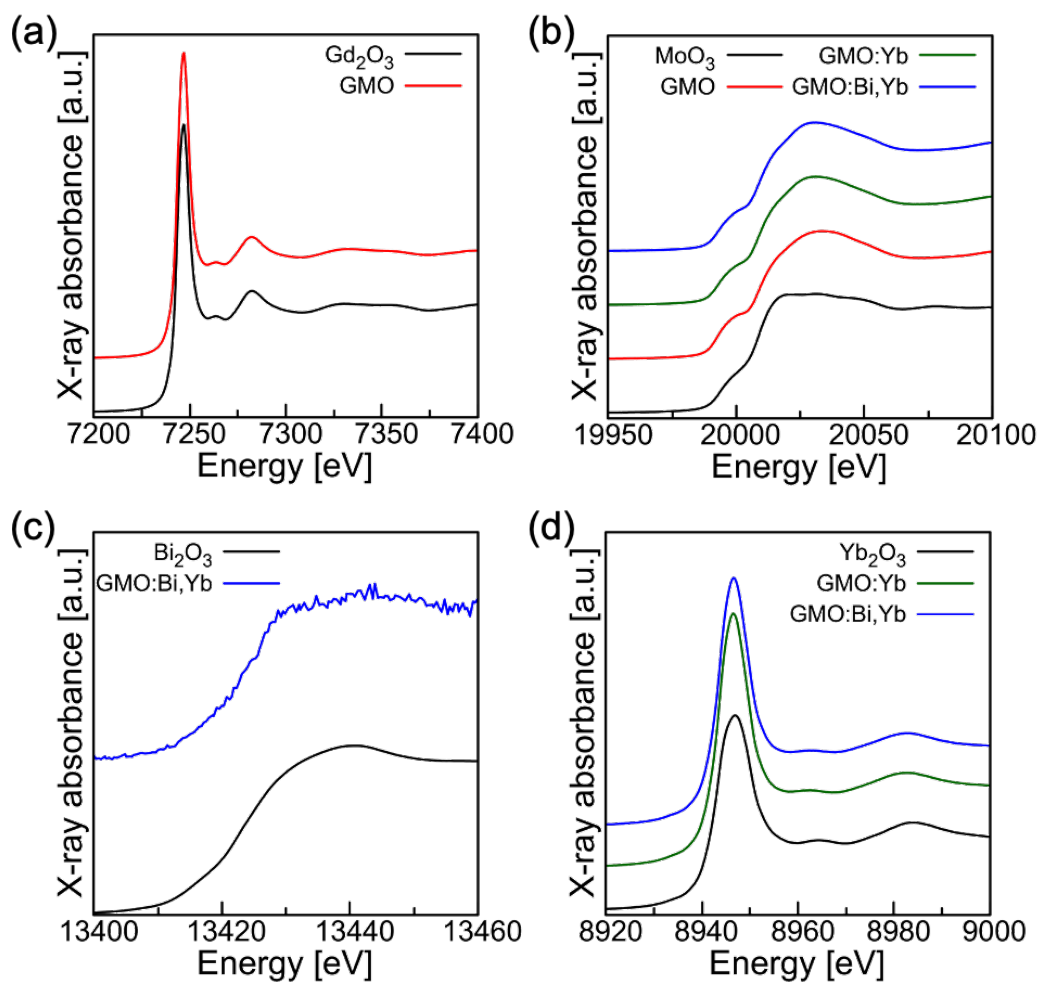


Figure S2. XANES spectra for all GMO nanophosphors of (a) Gd L_{3-} , (b) Mo K -, (c) Bi L_{3-} , and (d) Yb L_{3-} edge with the reference samples (Gd_2O_3 , MoO_3 , Bi_2O_3 , and Yb_2O_3).

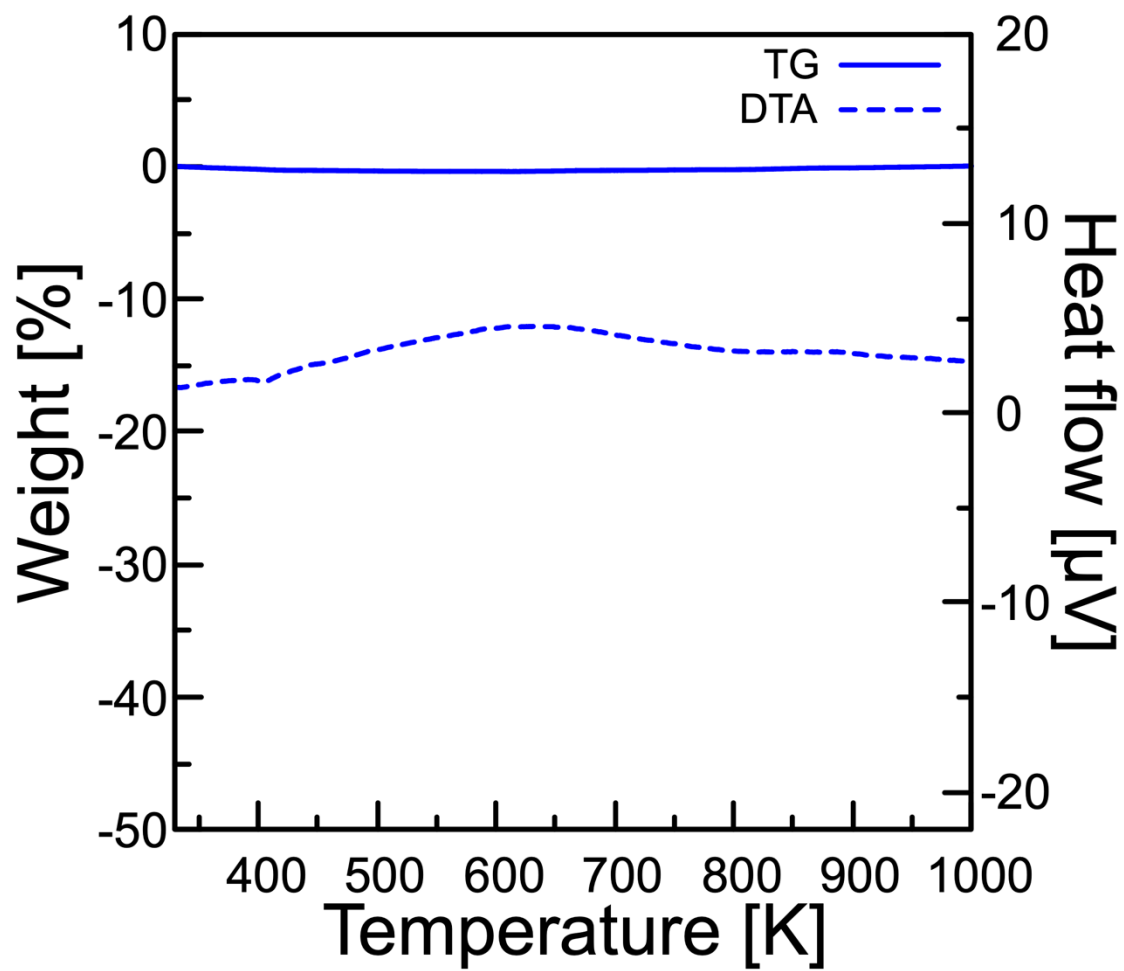


Figure S3. TG-DTA curve for GMO:Bi,Yb, and from 330 K to 1000 K under ambient air.

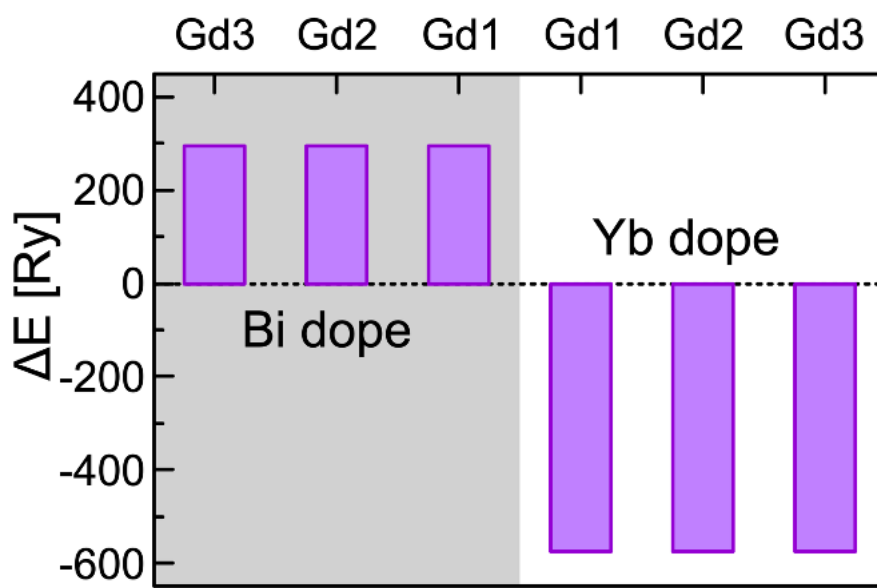


Figure S4. ΔE values calculated from the total energy obtained after structural relaxation.

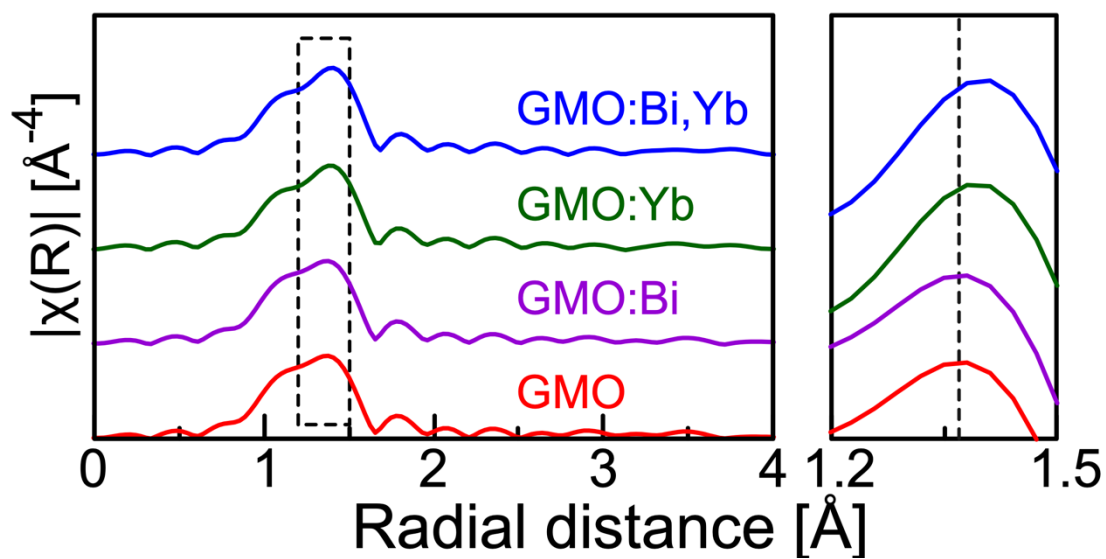


Figure S5. Fourier transformed EXAFS radial distribution function spectra of Mo K-edge in all GMO nanophosphors.

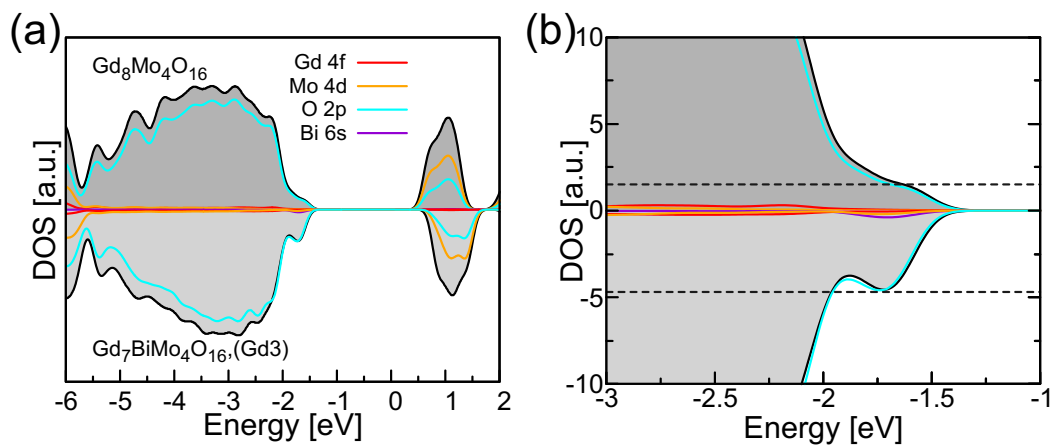


Figure S6. (a) DOS/pDOS of GMO:Bi substituted in Gd₃ site, and (b) enlarged one.

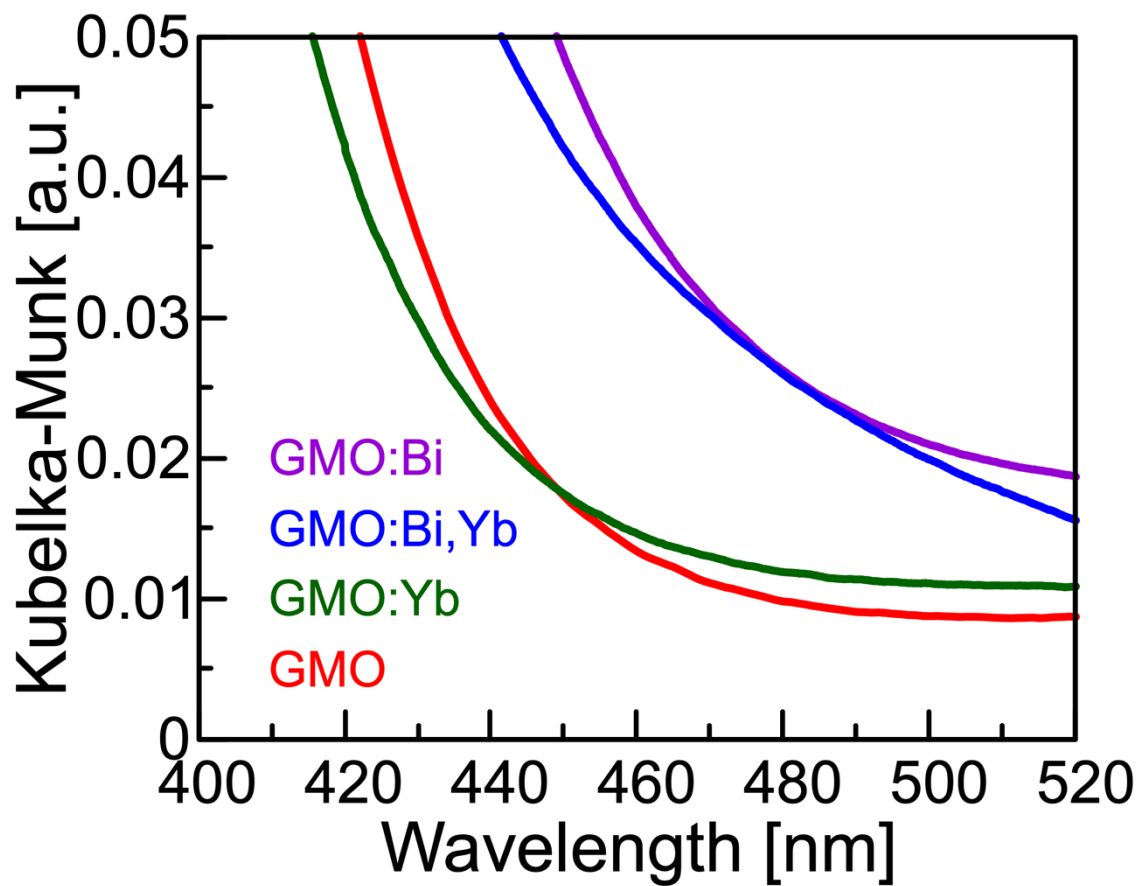


Figure S7. Kubelka-Munk spectra of all GMO nanophosphors around 500 nm.

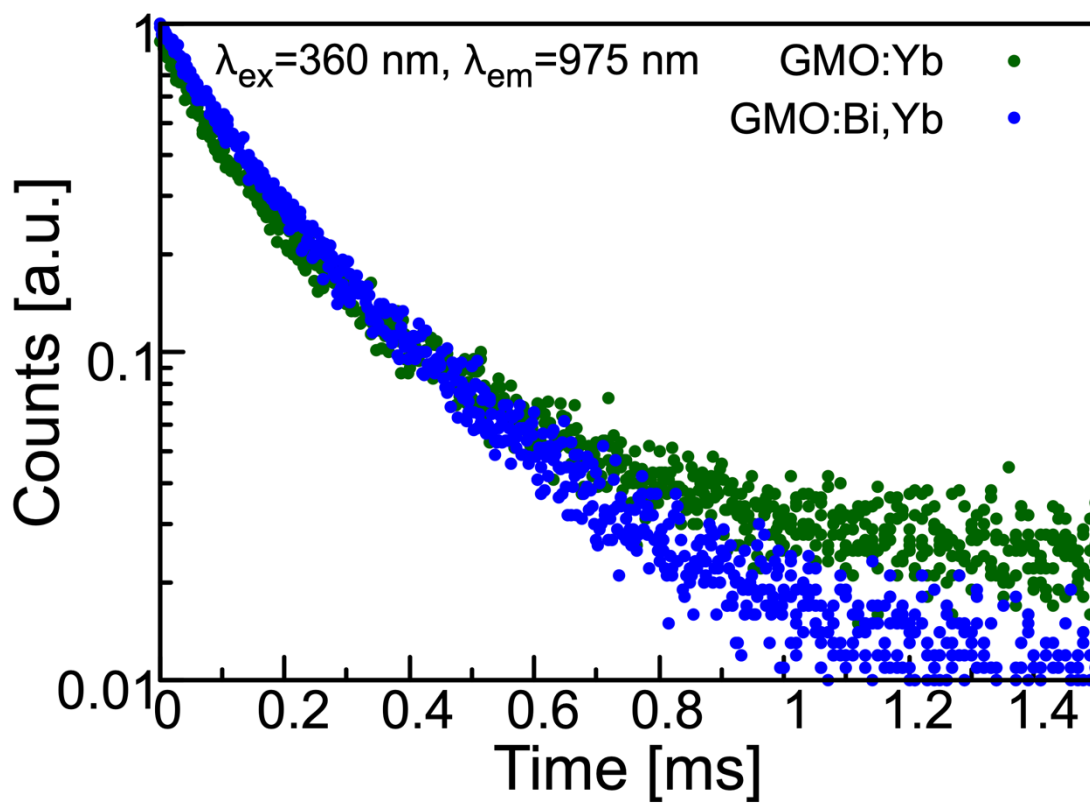


Figure S8. Decay curves of GMO:Yb and GMO:Bi,Yb at 300 K ($\lambda_{\text{ex}}=360 \text{ nm}$ and $\lambda_{\text{em}}=975 \text{ nm}$).

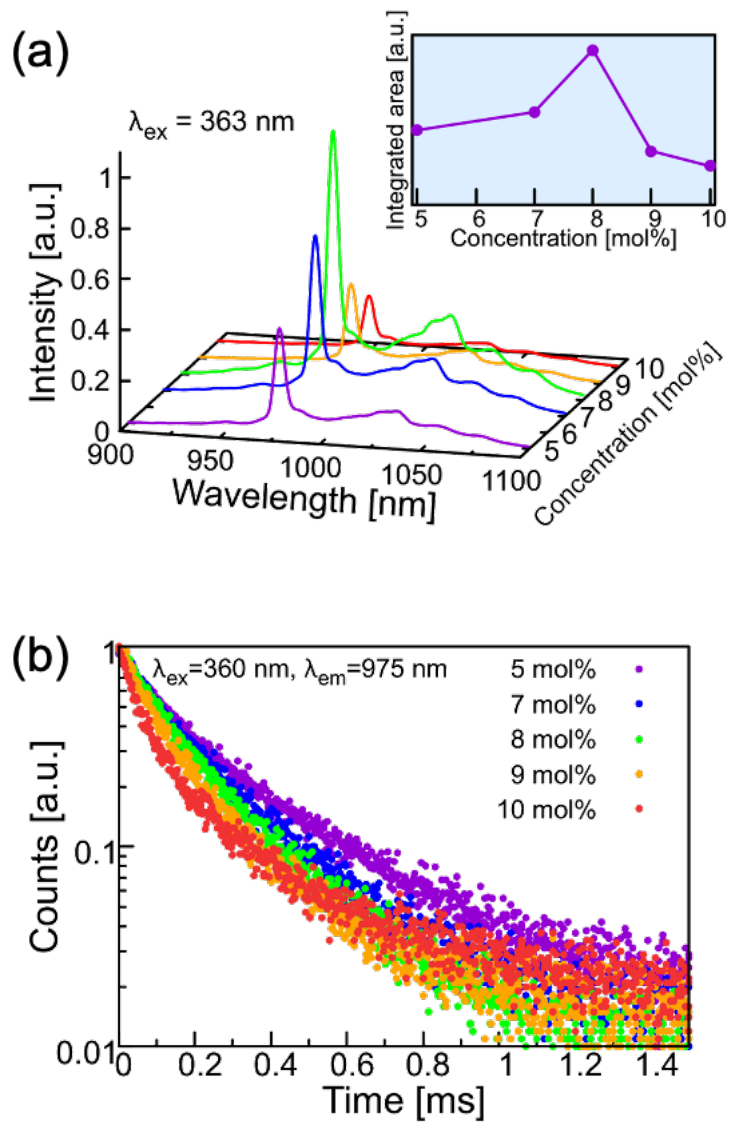


Figure S9. (a) PL spectra ($\lambda_{\text{ex}} = 363 \text{ nm}$) and (b) decay curve ($\lambda_{\text{ex}} = 360 \text{ nm}$ and $\lambda_{\text{em}} = 975 \text{ nm}$) of $\text{GMO:Bi}_y\text{Yb}$ ($y = 5, 7, 8, 9,$ and 10 mol\%) nanoposphors at 300 K .

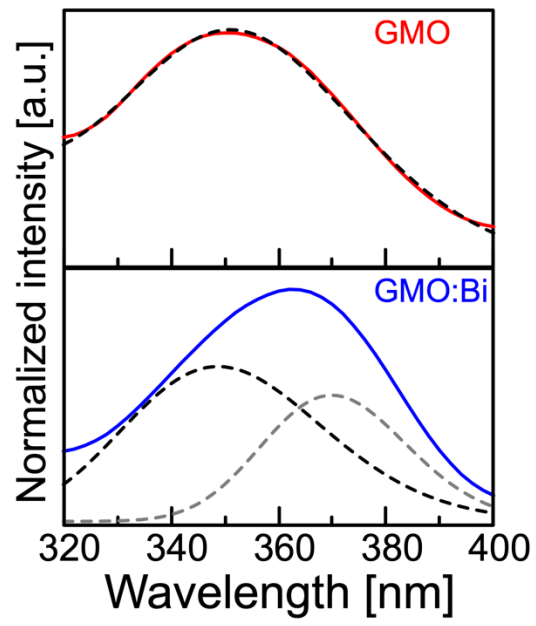


Figure S10. Gaussian fit of PLE spectra for GMO and GMO:Bi at 77 K.

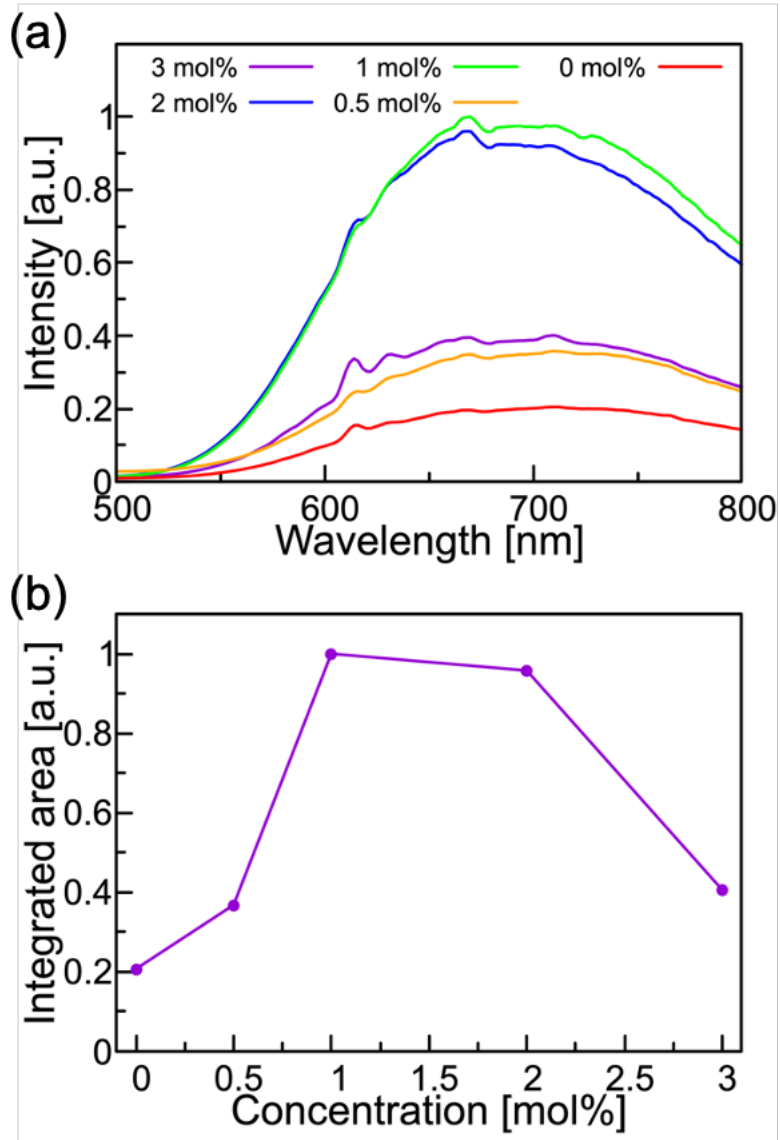


Figure S11. (a) PL spectra ($\lambda_{\text{ex}} = 360$ nm) and (b) integrated intensity of GMO:xBi, ($x = 0, 0.5, 1, 2,$ and 3 mol%) nanophosphors at 77 K.

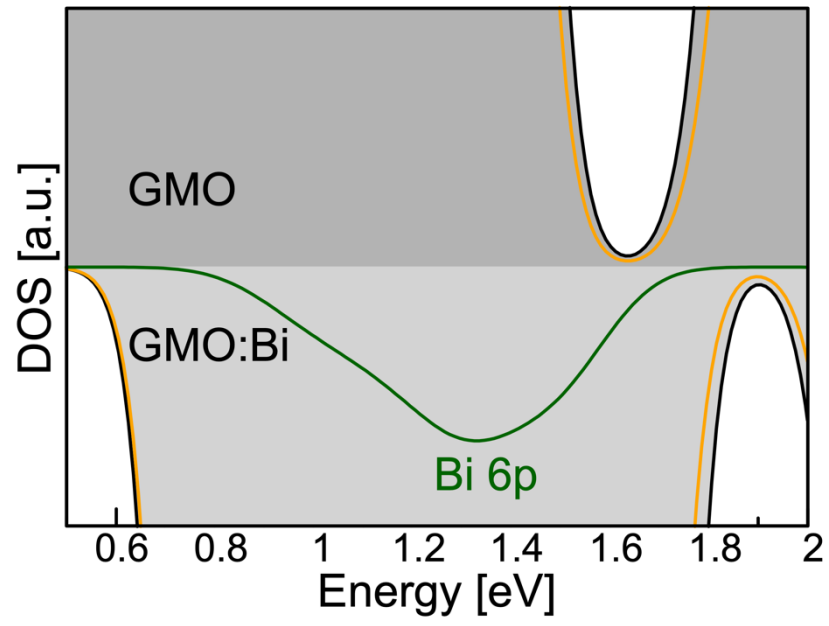


Figure S12. Enlarged DOS/pDOS of GMO:Bi substituted in Gd1 around conduction band minimum.

Table S1. Molar ratios of Gd/Bi/Yb for all GMO nanophosphors calculated from XPS.

	GMO	GMO:Bi	GMO:Yb	GMO:Bi,Yb
Gd [mol%]	100	94.6	96.2	90.4
Bi [mol%]	0	5.33	-	7.92
Yb [mol%]	0	-	3.80	1.67

Table S2 Lattice parameters for each GMO nanophosphor refined by Rietveld analysis.

	GMO	GMO:Bi	GMO:Yb	GMO:Bi,Yb
a [Å]	16.54(1)	17.13(1)	17.13(1)	16.508(4)
b [Å]	11.183(6)	10.796(4)	10.741(5)	11.161(3)
c [Å]	5.408(3)	5.417(5)	5.395(2)	5.394(1)
β [°]	108.50(3)	108.50(7)	108.50(3)	108.247(1)
V [Å ³]	949(1)	950(1)	941.2(8)	942.7(4)
R_{wp} [%]	9.788	10.48	8.252	9.133
R_p [%]	7.463	7.710	6.234	7.218
S	3.013	2.727	1.729	2.231

Table S3. Lattice parameters and average bond length for each GMO nanophosphor refined by Rietveld analysis.

		CIF	DFT	Rietveld
Lattice parameter	a [Å]	9.959	9.904	10.004
	b [Å]	9.959	9.903	10.004
	c [Å]	5.418	5.393	5.412
	α [°]	105.06	104.78	105.25
	β [°]	105.06	104.79	105.25
	γ [°]	68.223	68.292	67.877
Average bond length	Gd1-O	2.449	2.430	2.451
	Gd2-O	2.442	2.417	2.425
	Gd3-O	2.405	2.395	2.406
	Mo-O	1.884	1.876	1.896

Table S4. Calculated total energy after structural relaxation and ΔE values.

		Total energy [Ry]	ΔE [Ry]
	GMO	-11949.258	-
	Gd1	-11653.825	295.433
Bi	Gd2	-11653.826	295.432
	Gd3	-11653.837	295.421
	Gd1	-12525.176	-575.918
Yb	Gd2	-12525.160	-575.902
	Gd3	-12525.160	-575.902

Table S5. Fitting parameters of decay curves for GMO:Yb and GMO:Bi,Yb measured at 300 K.

Sample	τ_1 [μs]	τ_2 [μs]	A_1 [-]	A_2 [-]	τ_{ave} [μs]
GMO:Yb	58.3	239	461	454	203
GMO:Bi,Yb	97.3	265	583	410	207

Table S6. Fitting parameters of decay curves for $\text{GMO:Bi}_y\text{Yb}$ ($y= 5, 7, 8, 9,$ and 10 mol%) measured at 300 K.

y [mol%]	τ_1 [μs]	τ_2 [μs]	A_1 [-]	A_2 [-]	τ_{ave} [μs]
5	95.3	340	441	496	291
7	102	299	557	420	238
8	97.3	265	583	410	207
9	73.4	229	611	402	178
10	50.1	265	674	302	201

Table S7. Fitting parameters of decay curves for $\text{GMO:Bi}_y\text{Yb}$ ($y = 0, 0.5, \text{ and } 1$ mol%) nanophosphors measured at 77 K ($\lambda_{\text{ex}} = 360$ nm and $\lambda_{\text{em}} = 670$ nm).

y [mol%]	τ_1 [μs]	τ_2 [μs]	A_1 [-]	A_2 [-]	τ_{ave} [μs]
0	6.61	34.3	0.0240	0.00378	19.1
0.5	3.11	28.8	0.0322	0.00305	15.1
1	2.28	23.2	0.0375	0.00290	11.5